Cryogenics 51 (2011) 132–138

Contents lists available at ScienceDirect

Cryogenics

journal homepage: www.elsevier.com/locate/cryogenics

Heat exchanger for subcooling liquid nitrogen with a regenerative cryocooler

Ho-Myung Chang *, Seung Hoon Ryu

Hong Ik University, Seoul 121-791, Republic of Korea

ARTICLE INFO

Article history:
Received 14 September 2010
Received in revised form 2 December 2010
Accepted 25 December 2010
Available online 1 January 2011

Keywords:
Nitrogen (B)
Subcooled liquid (C)
Heat exchanger (E)
Regenerative cryocooler (E)

ABSTRACT

A heat exchanger for continuously subcooling liquid nitrogen in contact with a regenerative cryocooler is analytically investigated as a next step of our recent experimental works. Since the coldhead of regenerative cryocooler has a limited surface area, a cylindrical copper cup is attached as extended surface, and a tube for liquid flow is spirally wound and brazed on the exterior surface of cylinder. Different sizes of heat exchangers are fabricated and tested with a single-stage GM cooler to cool liquid nitrogen from 78 K to 66 K. Analytical model is developed for the heat exchanger effectiveness and thermal resistance, and the results are compared with the experimental data. It is concluded that there exists an optimum for the height and diameter of cylindrical heat exchanger to maximize the cooling rate with a given unit of cryocooler.

1. Introduction

Subcooled liquid nitrogen is a common coolant in HTS (high temperature superconductor) power systems [10], including superconducting transmission cable [8], superconducting fault current limiter [5,6,12], or superconducting power transformer [3,13,14]. The main reason for using subcooled liquid in high-voltage systems is to suppress bubbles [11] that may be generated from external or internal heat source, because bubbles play a critical role in deteriorating the electrical insulation of liquid. In addition, it was reported that the temperature of HTS elements are spatially more uniform [9] and can be recovered more promptly from quench in subcooled liquid than in boiling liquid [4]. Fig. 1 shows the typical region of subcooled liquid for HTS power applications on phase diagram of nitrogen. For safe operation, the degree of subcooling (below its boiling temperature) is 10 K or greater, and liquid is pressurized to 300–500 kPa.

One of simple and convenient methods to maintain the subcooled state is to employ a cryocooler in so-called natural convection system [5–7,9,12]. With an extended cold surface thermally anchored to the coldhead of cryocooler, liquid nitrogen is actively circulated by natural convection, achieving a uniform cooling over the entire liquid-filled space. In some cases, however, the pumped circulation of liquid nitrogen is indispensible, because the internal thermal load (e.g. ac loss) is excessive as in HTS power transformer, or the cooling load is widely distributed as in HTS transmission cable. A heat exchanger is necessary to continuously absorb heat from the liquid stream and transfer it to the cryocooler, since any regenerative type (Stirling, GM, pulse tube) of cryocooler has a limited area of cold surface.

A prototype of pump-circulated system with subcooled liquid nitrogen was previously constructed and demonstrated for HTS power transformer by Yoshida et al. [14]. The system consisted of two cryostats; one for HTS windings and the other for pump unit. The pump unit had a cryogenic liquid pump and two GM coolers connected in parallel to produce subcooled liquid at 64 K and supply it to the HTS windings through a transfer tube. On the coldhead of each GM cooler, a heat exchanger made of copper cylinder was attached so that liquid nitrogen could be cooled through copper tube spirally wound on the cylinder. Recently, the present authors published an experimental work to investigate the effect of heat exchanger size. Several different sizes of heat exchangers were fabricated and tested with a commercial GM cooler to subcool liquid nitrogen from 78 K to 65–70 K [7]. It was demonstrated that the size of cylindrical heat exchanger could be optimized to achieve the maximum cooling of liquid nitrogen.

As a next step of the experimental study, this paper intends to develop an analytical method, with which the experimental results can be clearly explained and an optimal size of heat exchange can be determined for use in other systems. Towards this objective, the experiment is briefly summarized with some additional results, and then the heat exchanger equations are formulated and analytically solved. The expressions to calculate the heat exchanger effectiveness and subcooling rate are derived by taking into account the thermal resistance between heat exchanger and coldhead, and the cooling capacity of cryocooler.

* Corresponding author. Tel.: +82 2 320 1675; fax: +82 2 322 7003.
E-mail address: hmchang@hongik.ac.kr (H.-M. Chang).

0011-2275/$ - see front matter © 2010 Elsevier Ltd. All rights reserved.
doi:10.1016/j.cryogenics.2010.12.010

Nomenclature

B	dimensionless convection-conduction number (–)
C	specific heat of liquid nitrogen (J/kg K)
c	constants in general solutions of differential equations (–)
D	diameter of cylinder (m)
d	diameter of tube (m)
H	height of cylinder (m)
h	convective heat transfer coefficient (W/m^2 K)
k	thermal conductivity (W/m K)
$\dot{m}$	mass flow rate (kg/s)
N	dimensionless number of transfer unit (–)
p	pitch of spiral tube winding (m)
Pr	Prandtl number (–)
Q	dimensionless heat leak number (–)
q	heat transfer or cooling rate (W)
q''	heat leak from surrounding per unit area (W/m^2)
R	thermal resistance (K/W)
Re	Reynolds number (–)
T	temperature (K)
t	thickness of tube wall (m)
x	spiral distance along winding tube (m)
z	axial distance from bottom of cylinder (m)

Greek letters

δ	thickness of cylinder or top plate (m)
ε	heat exchanger effectiveness (–)
θ	dimensionless temperature (–)
ζ	dimensionless axial distance of cylinder (–)

Subscripts

0	top edge of cylinder
1	contact position of top plate and coldhead
c	contact resistance
CH	coldhead of cryocooler
Cu	copper cylinder
cyl	cylinder
e	exit of liquid nitrogen
i	inlet of liquid nitrogen or inner surface
LN	liquid nitrogen
min	minimum cooling temperature of cryocooler
o	outer surface
top	top plate

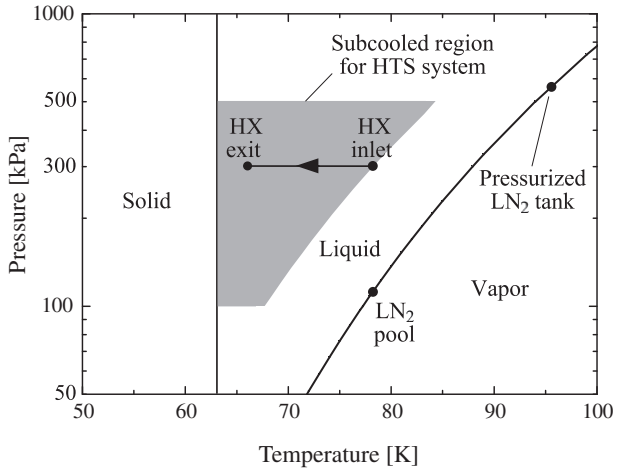

Fig. 1. Subcooled liquid region for HTS power applications and experimental subcooling process on phase diagram of nitrogen.

2. Experiment

Fig. 2 shows schematic diagram and photograph of heat exchanger system under investigation. A copper cylinder (diameter D, height H, thickness δ_{cyl}) is welded with a top plate (thickness δ_{top}), forming a "cup" shape (upside down) of extended surface. On external surface of the cylinder, a copper tube (diameter d, wall thickness t) is spirally wound and brazed with an axial pitch p. The top plate is bolt-jointed concentrically to the coldhead (diameter D_{CH}) of cryocooler. Liquid nitrogen enters the tube at bottom (temperature T_i) and exits at top (temperature T_e).

Fig. 3 is the simplified schematic of experimental apparatus. A single-stage GM cooler (Cryomech Model AL300) assembled with test heat exchanger is mounted on the top of cryostat. Liquid nitrogen supplied from a pressurized container is pre-cooled through a long tube submerged in liquid nitrogen pool at 78 K. Liquid at the inlet of heat exchanger is maintained nearly at 300 kPa and 78 K, and subcooled to 65–70 K through the heat exchanger, as indicated by an arrow in Fig. 1. The surface of coldhead and heat exchanger is wrapped with foam or fiber insulator in order to avoid the

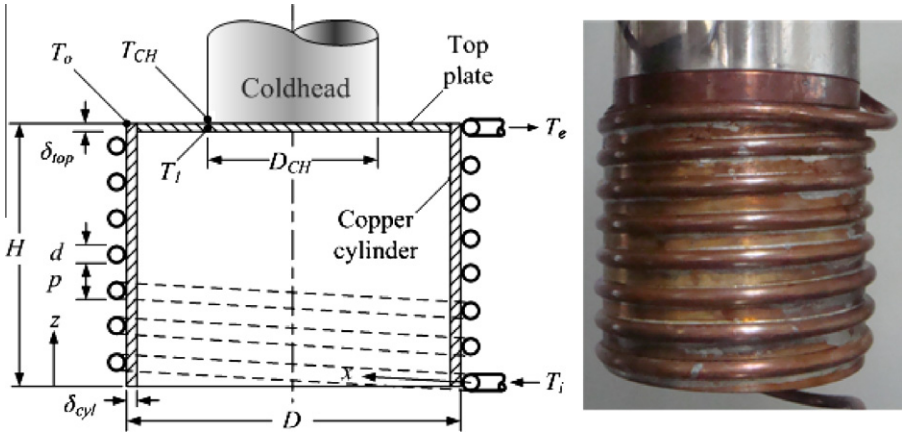

Fig. 2. Schematic diagram and photograph of heat exchanger system under investigation.

condensation of nitrogen vapor. The flow rate of liquid nitrogen is measured at room temperature after passing through a heated water bath. Temperature is measured with platinum resistors at the coldhead, the inlet and exit of heat exchanger. More temperature sensors are added lately at several axial locations of cylinder. Details of experimental set-up and procedure can be found in Chang et al. [7].

Five different sizes of heat exchanger are fabricated and tested. Each heat exchanger is identified with its diameter and height of cylinder in unit of mm. For example, D100-H50 indicated the heat exchanger with D = 100 mm and H = 50 mm. The experimental results for D100-H50, D100-H100, D100-H200, D50-H50, and D150-H50 are plotted in Fig. 4. Several new data from late experiment are added to the previous results. The cooling rate of liquid nitrogen is shortly calculated in terms of inlet and exit temperatures as

$$q_{LN} = \dot{m}_{LN} C_{LN} (T_i - T_e) \tag{1}$$

where $\dot{m}_{LN}$ and C_{LN} are the mass flow rate and specific heat of liquid nitrogen, respectively. Since T_i is 78 K in all tests, the cooling is more effective when $\dot{m}_{LN}$ is larger or T_e is smaller. It is clearly observed

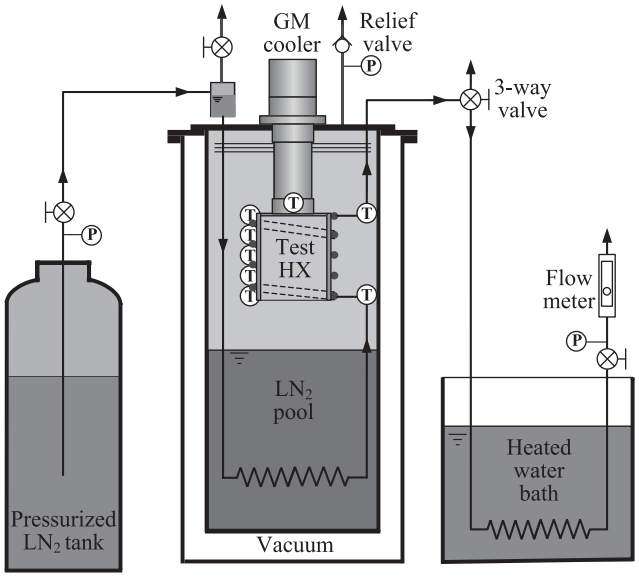

Fig. 3. Simplified schematic of experimental apparatus.

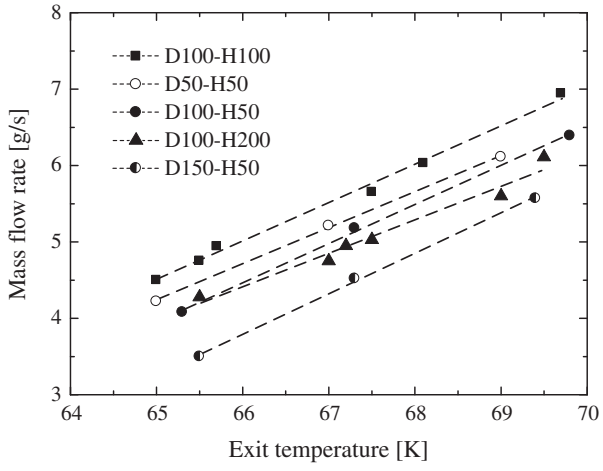

Fig. 4. Experimental results on mass flow rate of liquid nitrogen as a function of exit temperature for various sizes of heat exchanger.

that D100-H100 achieved the best cooling performance, and there exists an optimal size of heat exchanger with the specific cryocooler [7]. A systematic and analytical method to determine the optimal size is sought for the efficient cryogenic design of pumped circulation system.

3. Heat exchanger analysis

3.1. Formulation

For the heat exchanger in Fig. 2, the temperature of liquid nitrogen (T_{LN}) and copper cylinder (T_{Cu}) can be determined by energy balance equations with boundary conditions

$$\dot{m}_{LN} C_{LN} \frac{dT_{LN}}{dx} + U\pi d(T_{LN} - T_{Cu}) = 0, \quad T_{LN}(0) = T_i \tag{2}$$

$$k_{Cu}\pi D\delta_{cyl}\frac{d^2T_{Cu}}{dz^2} + U\pi d(T_{LN} - T_{Cu})\frac{dx}{dz} + \pi D(q_o'' + q_i'') = 0$$
$$\frac{dT_{Cu}(0)}{dz} = 0, T_{Cu}(H) = T_0 \tag{3}$$

where x and z are the spiral distance along the tube and the axial distance along the cylinder, respectively, so the two coordinates are related as

$$dx = dz\sqrt{\left(\frac{\pi D}{p}\right)^2 + 1} \tag{4}$$

The overall heat transfer coefficient U between T_{LN} and T_{Cu} is based on the wetted area of liquid in tube. As the tube is silver-brazed on cylinder wall, the temperature difference between the tube and cylinder is negligibly small at the point of contact. On the other hand, the tube wall may have a considerable temperature gradient in peripheral direction. It is reasonable to consider the tube wall as a plate fin with length $\pi d/2$ (by symmetry) and thickness t. Thus, U is simply the convective heat transfer coefficient h multiplied by the fin efficiency [1].

$$U = \frac{\sqrt{2hk_{Cu}t}}{\pi d}\tanh\left(\pi d\sqrt{\frac{h}{2k_{Cu}t}}\right) \tag{5}$$

where

$$h = \frac{k_{LN}}{d}0.023\mathrm{Re}^{0.8}\mathrm{Pr}^{1/3} \tag{6}$$

since the liquid flow is turbulent in all experimental conditions. In Eq. (3), q_o'' and q_i'' are the heat leak per unit area from surrounding to outer and inner surface of cylinder, respectively. It is assumed that the wall thickness is much smaller than the diameter for cylinder and tube.

The formulation is simplified by defining dimensionless variables

$$\zeta = \frac{z}{H} \quad \theta(\zeta) = \frac{T(z) - T_0}{T_i - T_0} \tag{7}$$

where T_i is the inlet temperature of liquid nitrogen (the highest temperature) and T_0 is the cylinder temperature at the top edge (the lowest temperature in heat exchanger). In dimensionless form

$$\frac{d\theta_{LN}}{d\zeta} + 2N(\theta_{LN} - \theta_{Cu}) = 0 \quad \theta_{LN}(0) = 1 \tag{8}$$

$$\frac{d^2\theta_{Cu}}{d\zeta^2} + B^2(\theta_{LN} - \theta_{Cu}) + Q = 0 \quad \frac{d\theta_{Cu}(0)}{d\zeta} = 0, \quad \theta_{Cu}(1) = 0 \tag{9}$$

where N, B, and Q are dimensionless parameters defined as

$$N = \frac{UH\pi d}{2\dot{m}_{LN}C_{LN}}\sqrt{\left(\frac{\pi D}{p}\right)^2 + 1} \quad B^2 = \frac{UH^2 d}{k_{Cu}\delta_{cyl}D}\sqrt{\left(\frac{\pi D}{p}\right)^2 + 1}$$
$$Q = \frac{(q_o'' + q_i'')H^2}{k_{Cu}\delta_{cyl}(T_i - T_0)} \tag{10}$$

It is noted that N is considered the number of transfer unit that is widely used for heat exchanger analysis, and B and Q are the relative ratio of fluid convection and heat leak to cylinder conduction, respectively. In case that $D \gg p$ (as in experimental heat exchangers), N and B can be further simplified.

$$N \approx \frac{UHD\pi^2 d}{2\dot{m}_{LN}C_{LN}p} \quad B^2 \approx \frac{UH^2\pi d}{k_{Cu}\delta_{cyl}p} \tag{11}$$

3.2. Analytical solution

The dimensionless temperatures can be obtained in closed form, if three parameters are constant.

$$\theta_{LN}(\zeta) = c_1 + e^{-N\zeta}\left[c_2\cosh\left(\sqrt{N^2+B^2}\zeta\right) + c_3\sinh\left(\sqrt{N^2+B^2}\zeta\right)\right] + \frac{2NQ}{B^2}\zeta \tag{12}$$

$$\theta_{Cu}(\zeta) = c_1 + \frac{e^{-N\zeta}}{2N}\left[\begin{array}{l}\left(Nc_2 + \sqrt{N^2+B^2}c_3\right)\cosh\left(\sqrt{N^2+B^2}\zeta\right) \\ +\left(\sqrt{N^2+B^2}c_2 + Nc_3\right)\sinh\left(sqrtN^2+B^2\zeta\right)\end{array}\right] + \frac{Q}{B^2}(1+2N\zeta) \tag{13}$$

where

$$c_1 = 1 + \frac{4N^2Q}{B^4} \tag{14}$$

$$c_2 = -\frac{4N^2Q}{B^4} \tag{15}$$

$$c_3 = \frac{\left(N\cosh\sqrt{N^2+B^2} + \sqrt{N^2+B^2}\sinh\sqrt{N^2+B^2}\right)\frac{4N^2Q}{B^4} - 2\left(1 + \frac{4N^2+(1+2N)B^2}{B^4}Q\right)Ne^N}{\sqrt{N^2+B^2}\cosh\sqrt{N^2+B^2} + N\sinh\sqrt{N^2+B^2}} \tag{16}$$

The exactness of solutions can be confirmed in different ways. Eqs. (8) and (9) are solved by numerical methods (4th-order Runge–Kutta integration) for given values of three parameters (N, B, and Q), and the temperature distributions are compared with Eqs. (12) and (13), and also with the experimental data. Fig. 5 is an example of calculated temperature distributions with the measured temperature data from D100-H100 experiment. In the calculation, the boundary conditions are T_i = 78.0 K and T_0 = 66.4 K, and N and B are given as 1.61 and 3.15, respectively, which are the corresponding values of experiment. Q is taken as 0.14, with which the exit temperature T_e matches the experimental value 66.4 K. This means that the Q value is based on the averaged heat leak from surrounding to satisfy the energy balance. The curves denoted by analysis are plots of Eqs. (12) and (13), which exactly agree with the results of numerical calculation. The temperature distribution of cylinder is in a fairly good agreement with the experiment data.

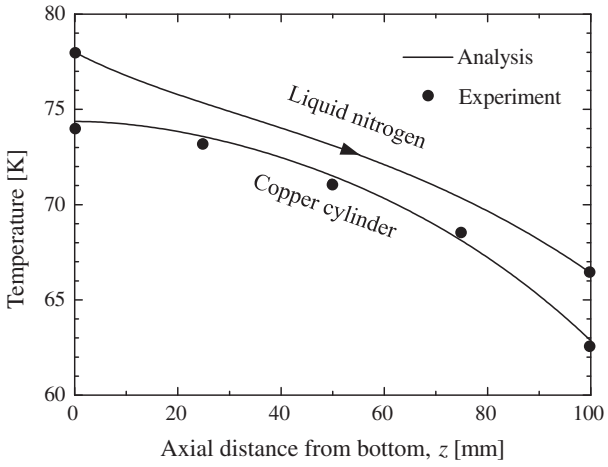

Fig. 5. Calculated temperature distribution of liquid nitrogen and copper cylinder in comparison with experimental data with D100-H100.

A reason for the small discrepancy is that the heat leak from surrounding (or the Q value) was not uniform over the axial length of cylinder in the experiment.

In an ideal case that the heat leak from surroundings is negligibly small or $Q = 0$, the three constants given by Eqs. (14)–(16) are reduced to

$$c_1 = 1 \quad c_2 = 0$$
$$c_3 = -\frac{2Ne^N}{\sqrt{N^2+B^2}\cosh\left(\sqrt{N^2+B^2}\right) + N\sinh\left(\sqrt{N^2+B^2}\right)} \tag{17}$$

so that Eqs. (12) and (13) may be simplified to

$$\theta_{LN}(\zeta) = 1 - \frac{2Ne^{N(1-\zeta)}\sinh\left(\sqrt{N^2+B^2}x\right)}{\sqrt{N^2+B^2}\cosh\left(\sqrt{N^2+B^2}\right) + N\sinh\left(\sqrt{N^2+B^2}\right)} \tag{18}$$

$$\theta_{Cu}(\zeta) = 1 - e^{N(1-\zeta)}\frac{\sqrt{N^2+B^2}\cosh\left(\sqrt{N^2+B^2}\zeta\right) + N\sinh\left(\sqrt{N^2+B^2}\zeta\right)}{\sqrt{N^2+B^2}\cosh\left(\sqrt{N^2+B^2}\right) + N\sinh\left(\sqrt{N^2+B^2}\right)} \tag{19}$$

3.3. Effectiveness

The effectiveness, ε, of heat exchanger shown in Fig. 2 is defined as the ratio of actual heat transfer rate to the maximum possible heat transfer rate [7].

$$\varepsilon \equiv \frac{T_i - T_e}{T_i - T_0} \tag{20}$$

where T_0 is the temperature of copper cylinder at the top edge. Therefore, the effectiveness can be derived from Eq. (12) as

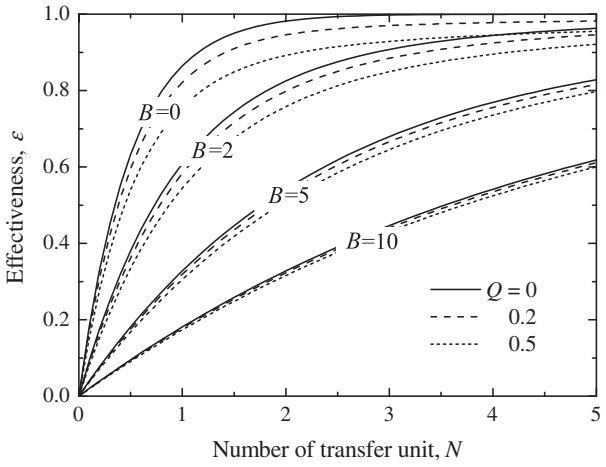

Fig. 6. Heat exchanger effectiveness as a function of N for various values of B and Q.

$$\varepsilon = 1 - c_1 - e^{-N}\left[c_2 \cosh\left(\sqrt{N^2+B^2}\right) + c_3 \sinh\left(\sqrt{N^2+B^2}\right)\right] - \frac{2NQ}{B^2} \tag{21}$$

which is plotted in Fig. 6 as a function of N for selected values of B and Q. The effectiveness increases with N in a similar pattern with general counter-flow heat exchanger. The effectiveness is higher, when B and Q are smaller. It can be also noted that the effect of Q is not so great for large values of B, which means that the effect of heat leak from surrounding is small when the wall conduction is dominant.

In the ideal case of $Q = 0$, Eq. (21) can be simplified

$$\varepsilon = \frac{2N}{\sqrt{N^2+B^2}\coth\left(\sqrt{N^2+B^2}\right) + N} \tag{22}$$

from Eq. (17), as lately derived by Barron [2] and the present authors. Some asymptotic behaviors for small N's or large N's are discussed by Barron [2].

4. Optimal size of heat exchanger

4.1. Thermal resistance model

The subcooling performance of liquid nitrogen is dependent on the thermal resistance between heat exchanger and coldhead, and the cooling capacity of cryocooler as well as the heat exchanger effectiveness. An equivalent thermal resistance model shown in Fig. 7 is taken for the system under investigation. Three thermal resistances should be considered in series for the model.

The first is a conduction resistance of top plate (header disc) of cylinder, if the cylinder diameter is greater than the coldhead diameter.

$$R_{top} = \begin{cases} 0 & D \le D_{CH} \\ \frac{\ln(D/D_{CH})}{2\pi k_{Cu}\delta_{top}} & D > D_{CH} \end{cases} \tag{23}$$

assuming that the temperature of top plate is uniform at T_1 over the area in contact with coldhead. The second is a contact resistance R_c [1] of the bolt-joint between the top plate and coldhead, which is generally dependent on the joint pressure and surface roughness of the mating surfaces. The third factor is the refrigeration capacity of cryocooler. As illustrated in Fig. 8 for the GM cryocooler (Cryomech AL300) used in the experiment, the cooling capacity is provided by the manufacturer as a function of coldhead temperature. For typical operating range between 40 K and 65 K, the capacity curve may be approximated with a reasonable accuracy by a linear function

$$q_{CH} \approx q_i \frac{T_{CH} - T_{\min}}{T_i - T_{\min}} \tag{24}$$

as indicated by the dotted line. In Eq. (24), q_i is the cooling capacity at T_i (the inlet temperature of liquid nitrogen), and $T_{\min}$ is the "extrapolated" minimum temperature with no load. According to Eq. (24), a thermal resistance, R_{CH}, is added in series between T_{CH} (coldhead temperature) and $T_{\min}$ in Fig. 8, as defined by

$$R_{CH} \equiv \frac{T_i - T_{\min}}{q_i} \tag{25}$$

Another factor to include in the thermal resistance model is the heat leak to top plate from surrounding.

$$q_{top} = \begin{cases} \int_0^{D/2} (q_i'' 2\pi r)dr & D \le D_{CH} \\ \int_{D_{CH}/2}^{D/2} (q_o'' 2\pi r)dr + \int_0^{D/2} (q_i'' 2\pi r)dr & D > D_{CH} \end{cases} \tag{26}$$

where q_o'' and q_i'' are the heat leak per unit area to outer (upper) and inner (lower) surface, respectively, similarly as before. For simplicity, it is assumed that this thermal load is added at temperature T_1 or

$$\frac{T_0 - T_1}{R_{top}} + q_{top} = \frac{T_1 - T_{CH}}{R_c} = \frac{T_{CH} - T_{\min}}{R_{CH}} = q_{CH} \tag{27}$$

Now, the overall energy balance is written

$$\dot{m}_{LN} C_{LN}(T_i - T_e) = q_{CH} - q_{cyl} - q_{top} \tag{28}$$

where

$$q_{cyl} = \pi D \int_0^H (q_o'' + q_i'')dz \tag{29}$$

By combining Eqs. (20), (27), and (28), the final expression is derived as

$$\dot{m}_{LN} = \frac{(T_i - T_{\min}) - (T_i - T_e)/\varepsilon - (R_{top} + R_c + R_{CH})q_{cyl} - (R_c + R_{CH})q_{top}}{C_{LN}(R_{top} + R_c + R_{CH})(T_i - T_e)} \tag{30}$$

for the mass flow rate of liquid nitrogen that can be continuously subcooled from T_i to T_e, for given cryocooler and heat exchanger. It is noted in Eq. (30) that the dimensional factors of heat exchanger, including the height (H) and diameter (D) of cylinder, affects the effectiveness (ε) as well as the thermal resistance (R_{top}) and heat leak from surrounding (q_{cyl} and q_{top}). Recalling that ε is a function of N, B, and Q, and the definition of N is involved of $\dot{m}_{LN}$, Eq. (30) should be solved by a few times of iterative calculations.

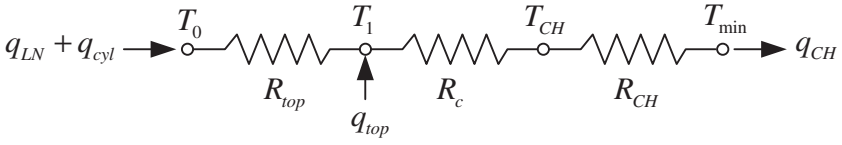

Fig. 7. Thermal resistance model for top plate, bolt-joint, and cryocooler capacity.

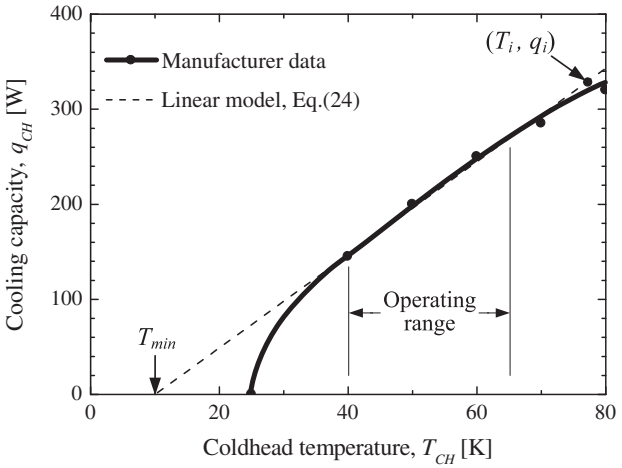

Fig. 8. Linear model for refrigeration capacity of GM cryocooler (Cryomech Model AL300) in operating temperature range.

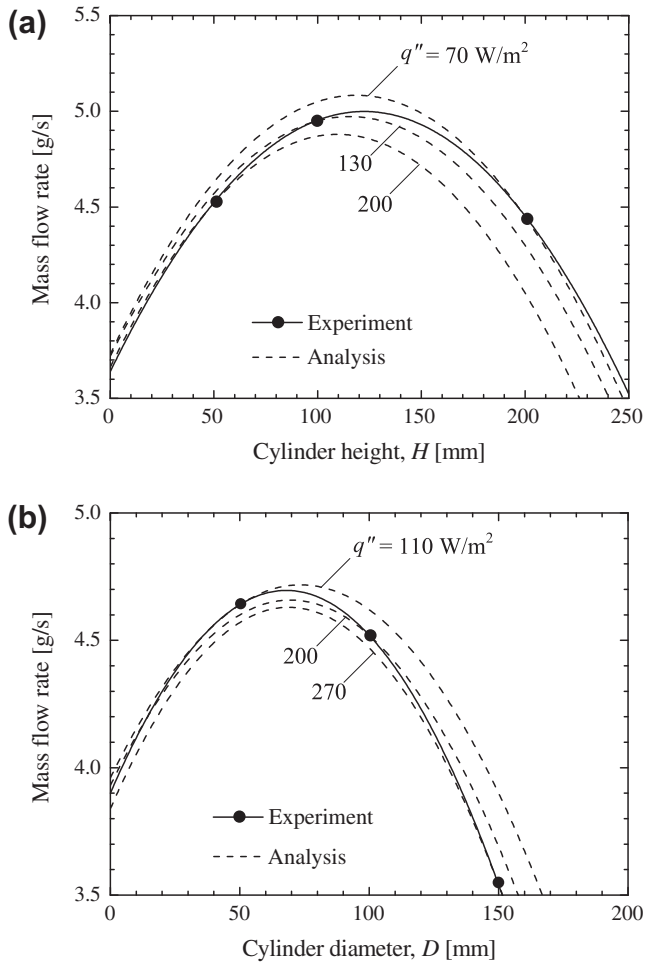

Fig. 9. Mass flow rate of liquid nitrogen cooled from 78 K to 66 K. (a) Effect of cylinder height. (b) Effect of cylinder diameter.

4.2. Results and discussion

In order to examine the effect of height (H) and diameter (D) of heat exchanger, the subcooling mass flow rate is calculated with Eq. (30) and plotted in Fig. 9a and b, respectively, in comparison with the experimental data. As listed in Table 1, the specifications

Table 1
Specifications and dimension of cryocooler, heat exchanger, and liquid nitrogen flow.

Cryocooler	Cooler type	Single-stage GM (Gifford–McMahon)
	Manufacturer	Cryomech, Inc.
	Model	AL300 (60 Hz)
	Cooling capacity	q_i = 310 W, T_{min} = 10 K (Linear model)
	Coldhead diameter	D_{CH} = 100 mm
Heat exchanger	Top plate (copper)	δ_{top} = 2 mm, R_c = 0.159 K/W^2 (Joint)
	Cylinder (copper)	δ_{cyl} = 2 mm
	Tube (copper)	d = 6.4 mm, t = 0.7 mm
	Tube winding (brazed)	p = 12.7 mm
Liquid nitrogen	Inlet temperature	T_i = 78.0 K
	Exit temperature	T_e = 66.0 K (interpolated)
	Properties	C_{LN} = 2024 J/kg K, k_{LN} = 0.14 W/m K, Pr = 2.23

and dimension of cryocooler, heat exchanger, and liquid nitrogen flow are taken from the experiment conditions. In all calculations, the inlet (T_i) and exit (T_e) temperatures of liquid nitrogen are fixed at 78.0 K and 66.0 K, respectively, as indicated in Fig. 1. The experimental points shown in Fig. 9a and b are estimated by interpolating the experimental data in Fig. 4. The only uncertain quantity in experiment is the heat leak (q'') to cylinder and top plate from surrounding. Thus, the analytical results are plotted with different values of $q''(=q_i''=q_o'')$ and compared with the experimental data represented by the solid interpolating curves.

Fig. 9a clearly shows that there exists an optimal H (around 120 mm) that maximizes the subcooling flow rate in experiment and analysis. If height is shorter than the optimum, the subcooling performance is poor because of smaller cooling surface area. On the contrary, if height is longer than the optimum, the subcooling is also poor because of larger heat leak. Similarly, Fig. 9b also shows that there exists an optimal D (around 80 mm) that maximizes the subcooling flow rate in experiment and analysis The main reason for the small discrepancy between experiment and analysis is the amount of q'', which was assumed to be a constant (averaged) value in the analysis, but varied significantly in the experiment. An interesting feature is to observe that q'' is larger when H is smaller or D is larger. This appears to be reasonable, because the inner surface of cylinder and top plate is more widely open to surrounding when H is smaller or D is larger.

Fig. 10 is a two-dimensional plot that illustrates the effect of H and D at the same time. The closed loops are contours of subcooling mass flow rate, which are calculated for the same experimental conditions and q'' = 120 W/m^2 rate. The vertical line

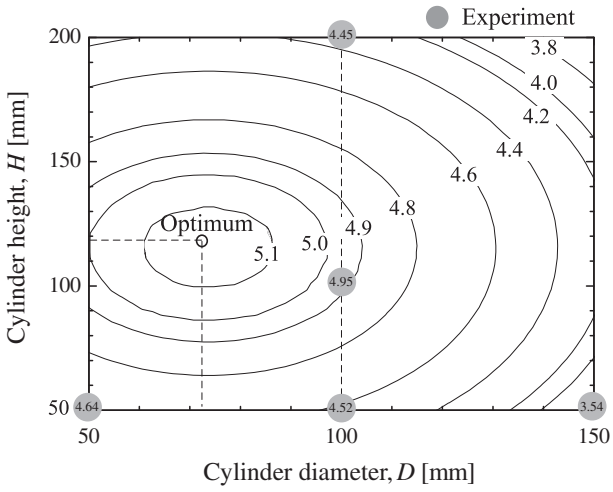

Fig. 10. Contours of mass flow rate of liquid nitrogen on cylinder height-diameter diagram (q'' = 120 W/m^2).

at $D = 100$ mm and the horizontal line at $H = 50$ mm represent Fig. 9a and b, respectively. Even though the largest subcooling rate was 5.0 g/s in the experiment, the maximum of 5.19 g/s is expected if the size of heat exchanger is optimized at $D = 118$ mm and $H = 73$ mm. The heat exchanger effectiveness and thermal resistance model developed in this study are useful for determining the optimal size of heat exchanger to take the best use of refrigeration capacity of any cryocooler.

5. Conclusions

An analytical method is successfully developed to predict the cooling rate of liquid nitrogen with heat exchanger in thermal contact with a regenerative cryocooler. The analysis includes an explicit form of expression for the heat exchanger effectiveness in terms of three dimensionless parameters (number of transfer unit N, convection-conduction ratio B, and heat leak ratio Q), and a thermal resistance model for the contact surfaces and refrigeration capacity of cryocooler. The analytical results are in fairly good agreement with experimental data. The developed method will be useful for anyone designing a heat exchanger in connection with a regenerative cryocooler.

Acknowledgments

This work is supported by 2010 Hong Ik University Research Fund. The authors wish to thank Prof. Randall F. Barron for discussion on the definition of heat exchanger effectiveness.

References

[1] Barron RF. Cryogenic heat transfer. Philadelphia: Taylor & Francis; 1999. p. 52–7.
[2] Barron RF. Personal Commun 2009.
[3] Chang HM, Choi YS, Van Sciver SW, Choi KD. Cryogenic cooling system for HTS transformers by natural convection of subcooled liquid nitrogen. Cryogenics 2003;43:589–96.
[4] Chang HM, Byun JJ, Choi JH, Ha CJ, Kim MJ, Kim HM, et al. Thermal diffusion of heat pulse in subcooled liquid nitrogen. Adv Cryogen Eng 2006;51:488–95.
[5] Chang HM, Kim MJ, Sim J, Lee BW, Oh IS. A compact cryocooling system with subcooled liquid nitrogen for small HTS magnets. IEEE Trans Appl Supercond 2008;18:1479–82.
[6] Chang HM, Lee GH, Sim J, Park KB, Oh IS, Song JB, et al. Two-stage cryocooling design for hybrid superconducting fault current limiter. IEEE Trans Appl Supercond 2010;20:2047–50.
[7] Chang HM, Ryu SH, Kim MJ. Performance of heat exchanger for subcooling liquid nitrogen with a GM cryocooler. Adv Cryogen Eng 2010;55:345–52.
[8] Chen RL, Henzler GW, Royal JH, Billingham JF. Reliability test of a 1-kW pulse tube cryocooler for HTS cable application. Adv Cryogen Eng 2010;55:727–35.
[9] Choi YS, Van Sciver SW, Chang HM. Natural convection of subcooled liquid nitrogen in a vertical cavity. Adv Cryogen Eng 2004;49:1091–8.
[10] Komarek P. Influence of HTS application on cryogenics now and in future. In: Proceedings of 21st international cryogenic engineering conference, 2007. p. 5–12.
[11] Nam KW, Seok BY, Byun JJ, Chang HM. Suppression of bubbles in subcooled LN2 under heat impulse. Cryogenics 2007;47:442–9.
[12] Ohtani Y, Yazawa T, Kuriyama T, Nomura S, Ohkuma T, Hobara N, et al. Subcooled nitrogen cryostat for 66 kV/750 A superconducting fault current limiter magnet. Adv Cryogen Eng 2004;49:867–74.
[13] Suzuki Y, Yoshida S, Kamioka Y. Subcooled liquid nitrogen refrigerator for HTS power systems. Cryogenics 2003;43(10–11):597–602.
[14] Yoshida S, Ohashi K, Umeno T, Suzuki Y, Kamioka Y, Kimura H, et al. 1 Atm subcooled liquid nitrogen cryogenic system with GM-refrigerator for a HTS power transformer. Adv Cryogen Eng 2002;47:473–80.